Arteriosclerosis, Thrombosis, and Vascular Biology

BASIC SCIENCES

Rewiring Vascular Metabolism Prevents Sudden Death due to Aortic Ruptures—Brief Report

Jorge Oller, Enrique Gabandé-Rodríguez, Raquel Roldan-Montero, María Jesús Ruiz-Rodríguez, Juan Miguel Redondo, José Luís Martín-Ventura, María Mittelbrunn

BACKGROUND: The goal of this study was to determine whether boosting mitochondrial respiration prevents the development of fatal aortic ruptures triggered by atherosclerosis and hypertension.

METHODS: Ang-II (angiotensin-II) was infused in ApoE (Apolipoprotein E)-deficient mice fed with a western diet to induce acute aortic aneurysms and lethal ruptures.

RESULTS: We found decreased mitochondrial respiration and mitochondrial proteins in vascular smooth muscle cells from murine and human aortic aneurysms. Boosting NAD levels with nicotinamide riboside reduced the development of aortic aneurysms and sudden death by aortic ruptures.

CONCLUSIONS: Targetable vascular metabolism is a new clinical strategy to prevent fatal aortic ruptures and sudden death in patients with aortic aneurysms.

GRAPHIC ABSTRACT: A graphic abstract is available for this article.

Key Words: aortic aneurysm ■ aortic rupture ■ DNA, mitochondria ■ glycolysis ■ mitochondrial respiration ■ vascular metabolism

Aortic dissection is an acute disorder characterized by splitting of the aortic wall's layers, usually caused by a tear in the intimal layer causing bleeding between the layers. Aortic dissection triggers sudden, violent pain, and is immediately life-threatening because it can cause the aorta to rupture with extensive hemorrhage or can lead to acute loss of perfusion in various organs. Although some aortic ruptures occur without a preexisting aneurysm, the occurrence of an aortic aneurysm increases the risk of aortic rupture and sudden death.[1] Age is an important risk factor for aortic aneurysms and dissections (AADs). Other important risk factors are hypertension, dyslipidemia, and genetic disorders that involve the connective tissue, such as Marfan, Loeys-Dietz, or Ehlers-Danlos syndromes. Whereas hereditable-AAD is usually located in thoracic aorta and its incidence is estimated to be 5.9/100 000 a year,[2] atherosclerotic-AAD is a relatively common condition, located in the abdominal aorta, found in up to 8% of men aged >65 years, and is responsible for considerable cardiovascular morbidity and mortality.[3] It is becoming increasingly clear that changes in vascular metabolism compromise arterial homeostasis and function.[4–6] Vascular smooth muscle cells (VSMCs) from mouse models and patients with Marfan Syndrome, that course with hereditable-AAD, present mitochondrial dysfunction, and boosting mitochondrial function rapidly reverted aortopathy and the pathological transcriptional signature in these Marfan mice.[7] Moreover, some previous evidences point out that the mitochondrial function might be compromise in non hereditable-AAD.[8,9] In this work, we investigate whether boosting mitochondrial metabolism with NAD precursors could prevent sudden death due aortic rupture during atherosclerotic-AAD.

Correspondence to: Jorge Oller, PhD, Immunometabolism and Inflammation Laboratory, Centro de Biología Molecular Severo Ochoa, C/ Nicolás Cabrera 1, 28049 Madrid, Spain, Email jorge.oller@cbm.csic.es; or María Mittelbrunn, PhD, Immunometabolism and Inflammation Laboratory, Centro de Biología Molecular Severo Ochoa, C/ Nicolás Cabrera 1, 28049 Madrid, Spain, Email mmittelbrunn@cbm.csic.es

Supplemental Material is available at https://www.ahajournals.org/doi/suppl/10.1161/ATVBAHA.121.317346.

For Sources of Funding and Disclosures, see page 468.

Arterioscler Thromb Vasc Biol is available at www.ahajournals.org/journal/atvb

Nonstandard Abbreviations and Acronyms

AAA	abdominal aortic aneurysms
AAD	aortic aneurysms and dissection
Ang-II	angiotensin-II
ApoE	apolipoprotein E
BP	blood pressure
HIF1A	hypoxia-inducible factor 1-alpha
NAD	nicotinamide adenine dinucleotide
MT-CO1	mitochondrially encoded cytochrome C oxidase I
MT-ND1	mitochondrially encoded NADH: ubiquinone oxidoreductase core subunit 1
MYH11	myosin-11
SDHA	succinate dehydrogenase complex flavoprotein subunit A
SPP1	secreted phosphoprotein 1
TFAM	mitochondrial transcription factor a
VSMC	vascular smooth muscle cell

Highlights

- Mitochondrial respiration decreases in aortic vascular smooth muscle cells in humans and in a mouse model of atherosclerotic aortic aneurysms.
- Boosting mitochondrial respiration by nicotinamide riboside treatment prevents sudden death by aortic ruptures.
- Nicotinamide riboside treatment could be a therapeutic opportunity to manage aortic aneurysms and to prevent aortic ruptures.

MATERIALS AND METHODS

Mouse Strain and Animal Procedures

The ApoE (Apolipoprotein E)-deficient mice, B6.129P2-*Apoe*^{tm1Unc}/J (JAX stock No. 002052), in pure C57/BL6J background were obtained from Charles Rivers. To accelerate atherosclerosis and increase the rate of aortic ruptures, 12-week-old male mice were fed a western diet (high fat and cholesterol diet, SSNIFF-S9167-E011, Ssniff Spezialdiäten, Germany), 3 weeks prior and maintained to Ang-II (angiotensin-II) infusion. Only male mice were studied as females are protected from developing AAD.[10,11] Ang-II was dissolved in saline (Sigma-Aldrich) and infused at 1 µg/kg·min using subcutaneous osmotic minipumps (Model 2004, Alzet Corp.). Nicotinamide riboside ([NR] Novalix) was administered intraperitoneally at 1000 mg/kg in 0.9% NaCl every other day. Ascending aorta and suprarenal abdominal aorta were analyzed by echochardiography and histology within the same mice. Lethal aortic ruptures were confirmed by the presence of hemothorax or hemoabdomen after necropsy showing as described.[12] Mice were housed at the pathogen-free animal facility of the Centro Nacional de Investigaciones Cardiovasculares Carlos III and Centro de Biología Molecular Severo Ochoa following the animal care standards of the institution. Animal procedures were approved by the Centro Nacional de Investigaciones Cardiovasculares Carlos III and Centro de Biología Molecular Severo Ochoa—Universidad Autónoma de Madrid Ethics Committee and the Madrid regional authorities (ref. PROEX 283/16) and conformed with European Union Directive 2010/63EU and Recommendation 2007/526/EC regarding the protection of animals used for experimental and other scientific purposes, enforced in Spanish law under Real Decreto 1201/2005.

Blood Pressure and In Vivo Imaging

Arterial blood pressure (BP) was measured by the mouse tail-cuff method using the automated BP-2000 Blood Pressure Analysis System (Visitech Systems, Apex, NC). Mice were trained for BP measurements every day for 5 consecutive days. After the training period, BP was measured before treatment to determine the baseline BP values in each mouse cohort. BP measurements were recorded in mice located in a tail-cuff restrainer over a warmed surface (37 °C). Fifteen consecutive systolic and diastolic BP measurements were made, and the last 10 readings per mouse were recorded and averaged. For in vivo ultrasound images, the aortic diameter was monitored in isoflurane-anesthetized mice (2% isoflurane) by high-frequency ultrasound with a VEVO 2100 echography device (VisualSonics, Toronto, Canada) at 30-µm resolution. Maximal internal aortic diameters were measured at end of diastole using VEVO 2100 software, version 1.5.0.

Cell Procedures

Isolation and culture of primary mouse VSMCs were described in Oller et al. 2017[12]. The media from thoracic descending and abdominal aortas were digested with a solution of collagenase and elastase (Worthington Biochem) until a single-cell suspension was obtained. Culture and isolation of the human primary VSMCs were described in Guedj et al.[13] The media from human abdominal aortic tissues obtained from abdominal aortic aneurysms (AAAs) or organ donors was microdissected from the adventitia. Tissues were then cut into small fragments, and VSMCs were plated after 3 hours of digestion with 0.22 U/mg collagenase and 4.58 U/mg elastase for the media. Cells were then cultured in smooth muscle cell growth medium supplemented with plasmocin, fetal calf serum, epidermal growth factor, basic fibroblast growth factor, and insulin. Smooth muscle actin and calponin1 immunostaining was used for determination purity of the VSMCs cultures. All experiments with primary murine VSMCs were performed during first passage and for primary human VSMCs were performed during 3 to 4 passages. All cells were tested negative for mycoplasma.

Real-Time and Quantitative PCR

Aortas were extracted after perfusion with 5 mL saline solution, and the adventitia layer was discarded. Liquid nitrogen frozen tissue was homogenized using a cold mortar and an automatic bead homogenizer (MagNA Lyzer, Roche). Total RNA was isolated with Trizol (Life Technologies). Total RNA (1 µg) was first digested with DNAse and reverse-transcribed with Maxima First Strand cDNA Synthesis Kit (ThermoFisher). For analysis of mtDNA levels, total DNA from cells and tissues

was extracted with the SurePrep kit (Fisher Scientific) or Trizol, respectively, according to the manufacture's guidelines. DNA was amplified using primers specific for cytochrome mt-Co1 (mitochondrially encoded cytochrome c oxidase 1) and mitochondrial 16S rRNA, then normalized to B2M (β-2 macroglobulin) and H2K nuclear-encoded gene controls. Real-time quantitative PCR was performed with the primers indicated in Supplementary Table for Reagents. Quantitative PCR reactions were performed in triplicate with SYBR master mix (Promega), according to the manufacturer's guidelines. To examine probe specificity, we conducted a postamplification melting curve analysis. For each reaction, only 1 melting temperature peak was produced. The amount of target mRNA in samples was estimated by the 2—CT relative quantification method, using *B2M*, YWHAZ (tyrosine 3-monooxygenase/tryptophan 5-monooxygenase activation protein ζ), and PP1A (protein phosphatase 1 catalytic α) for normalization. Fold ratios were calculated relative to mRNA expression levels from controls.

Immunoblot

For western blot analysis, the medias from aortas were microdissected and isolated, homogenized (MagNA Lyzer, Roche) and lysed at 4 °C in radioimmunoprecipitation assay buffer containing protease and phosphatase inhibitors cocktail (Sigma). Proteins were separated by SDS-PAGE and transferred onto 0.45-µm pore size polyvinylidene fluoride membranes (Immobilon-P PVDF membrane; Millipore). Polyvinylidene fluoride membranes were blocked with TBS-T (50 mM Tris, 150 mM NaCl, and 0.1% Tween-20) containing 5% (wt/vol) milk. Membranes were incubated with primary antibodies indicated in Supplementary Table for Reagents, followed by TBS-T washes and incubation with HRP (horseradish peroxidase) conjugated secondary antibodies (GE Healthcare). The signal was visualized by enhanced chemiluminescence with Luminata Forte Western HRP Substrate (Millipore) and the ImageQuant LAS 4000 imaging system. The antibodies that were used are indicated in the table for reagents.

Extracellular Flux Analysis and Extracellular L-Lactate Determination

Oxygen consumption rates were measured in XF-96 Extracellular Flux Analyzers (Seahorse Bioscience) in 25 000 mouse or 50 000 human VSMCs. Cells were seeded in nonbuffered DMEM medium containing 25 mM glucose and 1 mM $CaCl_2$. Three measurements were obtained under basal conditions and on addition of oligomycin (1 mM), fluoro carbonyl cyanide phenylhydrazone (1.5 mM), and rotenone (100 nmol/L) + antimycin A (1 mM). Oxygen consumption rate measurements were normalized to protein cell extracts. Extracellular lactate determination was performed with single-use reagent strips for Accutrend Plus Lactate Pro (Roche), based on an enzymatic spectrophotometry system by lactate oxidase layer. We analyzed 20 µL of conditioned medium after 24 hours of culture. L-lactate concentration was normalized to total protein cell extracts.

Human Aortic Tissues

We used as control abdominal aortas human tissues macroscopically normal and devoid of early atheromatous lesions from deceased organ donors. Healthy human aortas (N=9) were sampled from deceased organ donors with the authorization of the French Biomedicine Agency (PFS 09-007). Nine samples of atherosclerotic-AAA walls were collected from patients without aortic genetic disorder that were undergoing surgical repair of AAA and were enrolled in the RESAA ("REflet Sanguin de l'évolutivité des Anévrysmes de l'aorte abdominale") protocol.[13] Age and sex of the patients is indicated in Table S1. Informed consent was given for the use of the human samples for research purposes. All of our human studies conformed to the principles outlined in the Declaration of Helsinki.

Immunohistochemistry

Human AAAs and control aortas were fixed in paraformaldehyde 3.7%. Samples were embedded in paraffin and sectioned at 6 µm. Sections were deparaffinized in xylene, hydrated in ethanol, and boiled to retrieve antigens (10 mM Citrate Buffer, pH 6). After blocking in 1% BSA, 5% Normal Goat Serum, and 5% Horse Serum in PBS Triton-x 0.05%, slides were incubated with primary antibodies indicated in the table of reagents overnight at 4 °C. After 3 washes with Triton-x 0.05%, slides were then incubated with the appropriate secondary antibodies (goat anti-mouse and goat anti-rabbit conjugated with horseradish peroxidase [HRP], Vector laboratories) at RT for 30 minutes and posterior 3 washes with PBS-Triton-x 0.05%. Substrate staining was developed with diaminobenzidine (Vector laboratories), and sections were counterstained with hematoxylin, dehydrated, and mounted in DPX (Fluka). Images were acquired under a Leica DM2500 microscope with 20× HCX PL Fluotar objective lenses and Leica Application Suite V3.5.0 acquisition software. At least 3 independent images in medial areas with a similar smooth muscle cell density were analyzed per specimen, and the mean per specimen is represented. For immunohistochemistry quantification staining, automated quantification of positive area within aortic media was performed by automatic threshold analysis of immunohistochemistry images in Image J/Fiji.

Statistical Analysis

Normality of data was checked using a Shapiro-Wilk test. *F*-test was used to assess the equality of variance assumption. Differences between 2 groups were assessed using the unpaired Student *t*-test, *t*-test with Welch correction for unequal variances, or Mann-Whitney *U* test, where appropriate. Differences in experiments with ≥3 groups were analyzed by 1-way, 2-way, and Tukey post hoc test, as appropriate. For all other analysis, GraphPad Prism software 9 was used. Statistical significance was indicated as $^{***}P<0.001$ and $^{****}P<0.0001$. Sample size was chosen empirically based on our previous experiences in the calculation of experimental variability; no statistical method was used to predetermine sample size. The numbers of animals used are described in the corresponding figure legends. All experiments were done with at least 3 biologic replicates. Experimental groups were balanced in terms of animal age and weight. Animals were genotyped before experiments and were all caged together and treated in the same way. Only male mice were studied as females are protected for aortic rupture.[10]

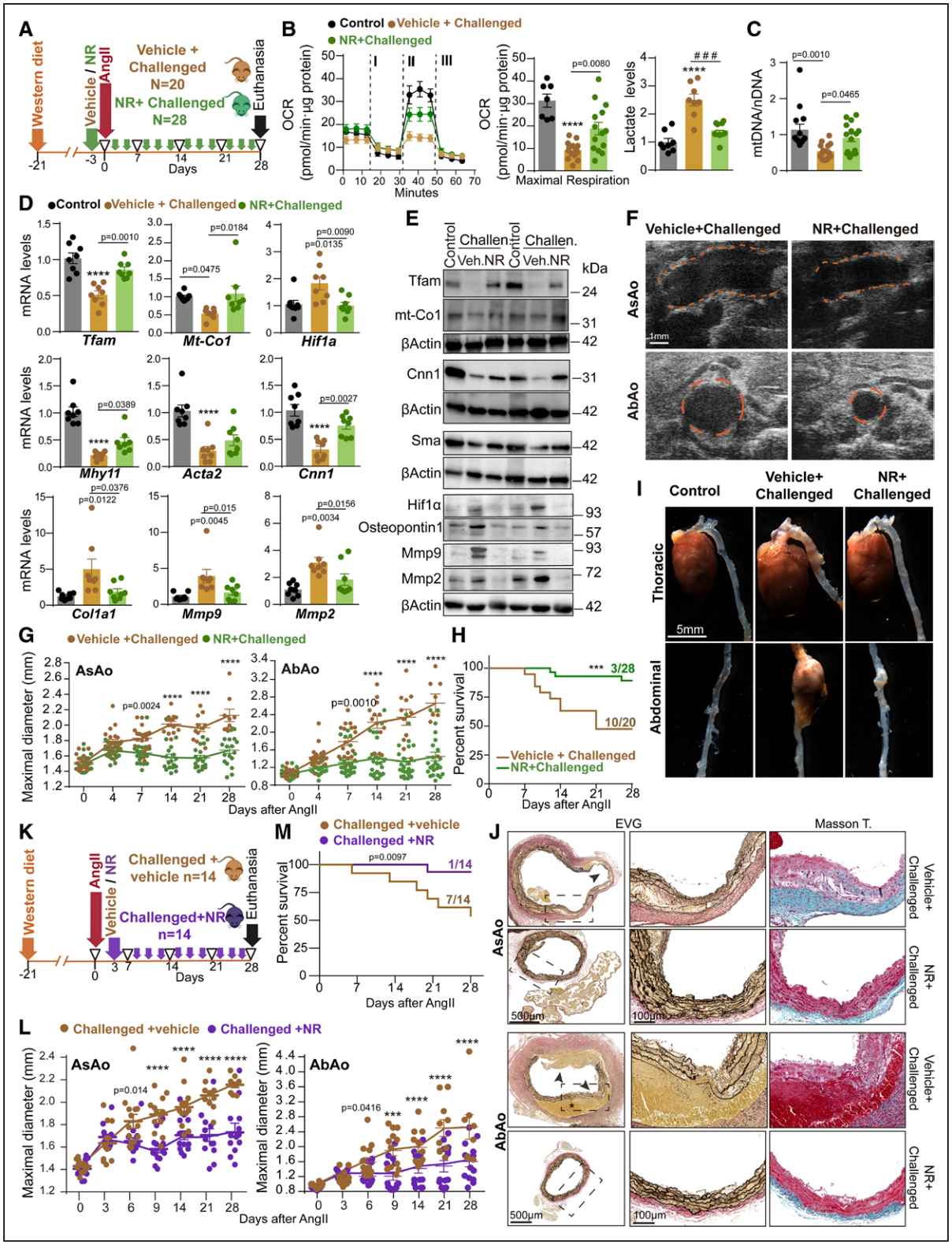

Figure 1. Nicotinamide riboside (NR) treatment prevents aortic ruptures and sudden death because of atherosclerotic aortic aneurysms.

A, Experimental design for the analysis of atherosclerotic aortic aneurysms in mice. **B**–**F**, Eight-wk-old male *Apoe*$^{-/-}$ mice were fed with western diet. Twenty-one days after, mice (challenged-mice) were infused with AngII for additional 28 d (1 µg/d×kg). Three days before AngII infusion, mice were treated (green arrowheads) with NR (1000 mg×kg each day; n=20) or vehicle (n=20). **B**, Oxygen consumption rate (OCR) (Seahorse Biosciences) in vehicle- and NR-treated VSMCs from challenged- and control-*Apoe*$^{-/-}$ mice at basal respiration and after addition of oligomycin (I) and fluoro carbonyl cyanide phenylhydrazone (II) to measure maximal respiration, (*Continued*)

RESULTS AND DISCUSSION

To investigate the potential benefit of boosting mitochondrial respiration in a mouse model of acute atherosclerotic aortic aneurysms and ruptures, ApoE-deficient mice were fed on a western diet for 3 weeks and infused with angiotensin-II for 28 days (challenged mice). In challenged mice, hypertension and hypercholesterolemia promote robust aneurysm development and lethal aortic ruptures.[14–16] Three days before Ang-II infusion, mice were intraperitoneally injected with the NAD^+-precursor NR (n=28) or with vehicle (n=20) (Figure 1A). Treatment with NR increased maximal oxygen consumption rate and decreased extracellular lactate levels in aortic VSMCs isolated from challenged-mice (Figure 1B). NR treatment also increased mitochondrial DNA (mtDNA) content (Figure 1C) and the expression levels of *Mt-Co1,* a gene encoded by the mtDNA (Figure 1D) in aortic extracts from Challenged-mice. In addition, NR treatment restored basal levels of the Tfam (mitochondrial transcription factor A), and Hif1α (Figure 1D and 1E), as well as proteins involved in the contractile-synthetic phenotype, such as Myh11 (Myosin-11), and Cnn1 or the extracellular proteins Col1a1, Spp1 (secreted phosphoprotein 1), Mmp9, and Mmp2 (Figure 1D and 1E). Moreover, NR-treatment tend to restore *Acta2* expression levels (Figure 1D and 1E).

Although NR treatment did not modify blood pressure (data not shown), it effectively prevented aortic dilation, medial degeneration, aortic aneurysm formation, and significantly reduced aortic lethal ruptures from 50% in Vehicle-Challenged mice (4 animals showed hemothorax, 6 showed hemoabdomen, 10 animals did not presented lethal aortic ruptures at the end of the experiment) to 12% in their NR-treated counterparts (1 animal with hemothorax, 1 with hemoabdomen, 1 with no apparent aortic aneurysm or rupture and 25 animals with no lethal aortic ruptures at the end of the experiment; Figure 1F through 1J).

To explore, not only the preventive, but also the curative potential of NR, we assessed whether NR was able to revert aortic aneurysms and reduce the risk of aortic rupture when the treatment starts after the onset of AAD. Therefore, we treated Challenged-mice with NR 3 days after Ang-II infusion (n=14 each group). NR treatment post-AngII infusion prevented the development of aortic dilation, aneurysms, and lethal aortic ruptures. We observed that treatment with NR after Ang-II infusion reduced the risk of lethal aortic ruptures from 50% to 7% (7 lethal aortic ruptures in mice treated with vehicle, 4 of them showing hemothorax, and 3 with hemoabdomen), whereas in the NR group only one mouse presented hemothorax (Figure 1K through 1M).

To extend the potential of boosting mitochondrial function to human abdominal atherosclerotic aortic aneurysm samples (AAA), we analyzed the expression of the mitochondrial proteins MT-ND1, SDHA (succinate dehydrogenase complex flavoprotein subunit A), MT-CO1, and TFAM in human-AAA-histological samples. While proteins related to mitochondrial respiration were decreased, we observed an increase of the pro-glycolytic transcription factor, HIF1A (hypoxia-inducible factor 1-alpha; Figure 2A and 2B). Moreover, VSMCs from AAA patients treated with NR for 5 days exhibited improved mitochondrial function (Figure 2C), correlating with a tendency to increase the mitochondrial-DNA levels (Figure 2D) and the expression of mitochondrial proteins TFAM, MT-CO1 by NR treatment (Figure 2E and 2F). Moreover, NR treatment significantly increased the expression of *MT-ATP6* and reduced the expression of genes encoding the extracellular remodeling proteins such as *MMP9, THBS1. ACAN* levels follow the same tendency (Figure 2E and 2F).

Although hereditable and atherosclerotic aneurysms have notably different aetiologies, they share common anatomical, histological, and molecular features. Anatomically, they are characterized by aortic enlargement. Histologically, they progress with a massive extracellular matrix remodeling and elastin degradation. Both conditions present alterations in angiotensin, TGF-β, ROS-associated molecular pathways, and enhanced metalloproteinase activity.[2,3] The central factor underlying these similarities is that both hereditable and atherosclerotic stem from the aberrant function of VSMCs. In this study, we provide further evidence that

Figure 1 Continued. followed by a combination of rotenone and antimycin A (III); and normalized extracellular lactate levels. **C**, qPCR analysis of relative mtDNA levels (*mt-Co1*) relative to nuclear DNA (*Actb*) content. **D**, RT-qPCR analysis of relative *Tfam, Mt-Co1, Myh11*, *Acta2*, *Cnn1 Col1a1*, *Mmmp9*, and *Mmp2* mRNA expression. **E**, Representative inmmunoblot analysis from aortic media extracts for Tfam, mt-Co1, Cnn1, Sma, Hif1a, Osteopontin1, Mmp9, Mmp2, in which each lane represents one mouse (n=6 each group); β-Actin was used for loading control. **F**, Representative ultrasound aortic images (VEVO 2100 echography device, VisualSonics) after 28 d of vehicle or NR treatment, discontinuous red lines mark the lumen boundary. **G**, Maximal ascending (AsAo) and abdominal (AbAo) aortic diameter, and (**H**) survival curve of challenged-mice. **I**, Representative macroscopic aortic images after 28 d of AngII infusion from animals of the same cohort showed in **F**. **J**, Representative elastin van-Gieson (EVG) and Masson's trichrome (Masson T) staining in AsAo and AbAo. Black arrows indicate aortic dissections, * indicate false lumen. **K**, Experimental design for the analysis of atherosclerotic aortic aneurysms in mice (**L**). Eight-wk-old male *Apoe*$^{-/-}$ mice were fed with western diet. Twenty-one days after, mice (challenged-mice) were infused with AngII for additional 28 d (1 μg/d×kg). Three days after AngII infusion, mice were treated (violet arrowheads) with NR (1000 mg×kg each day; n=14) or vehicle (n=14); **L**, Maximal ascending (AsAo) and abdominal (AbAo) aortic diameter and (**M**) survival curve of challenged-mice. Differences between the 3 groups were assessed by using 1-way ANOVA and a Tukey multiple comparisons test. Aortic diameters were assessed by using 2-way ANOVA and a Tukey multiple comparisons test. Survival curves (**M** and **H**) were assessed by log-rank (Mantel–Cox) test. ***P<0.001, ****P<0.0001 vs control; ###P<0.001 for vehicle vs NR.

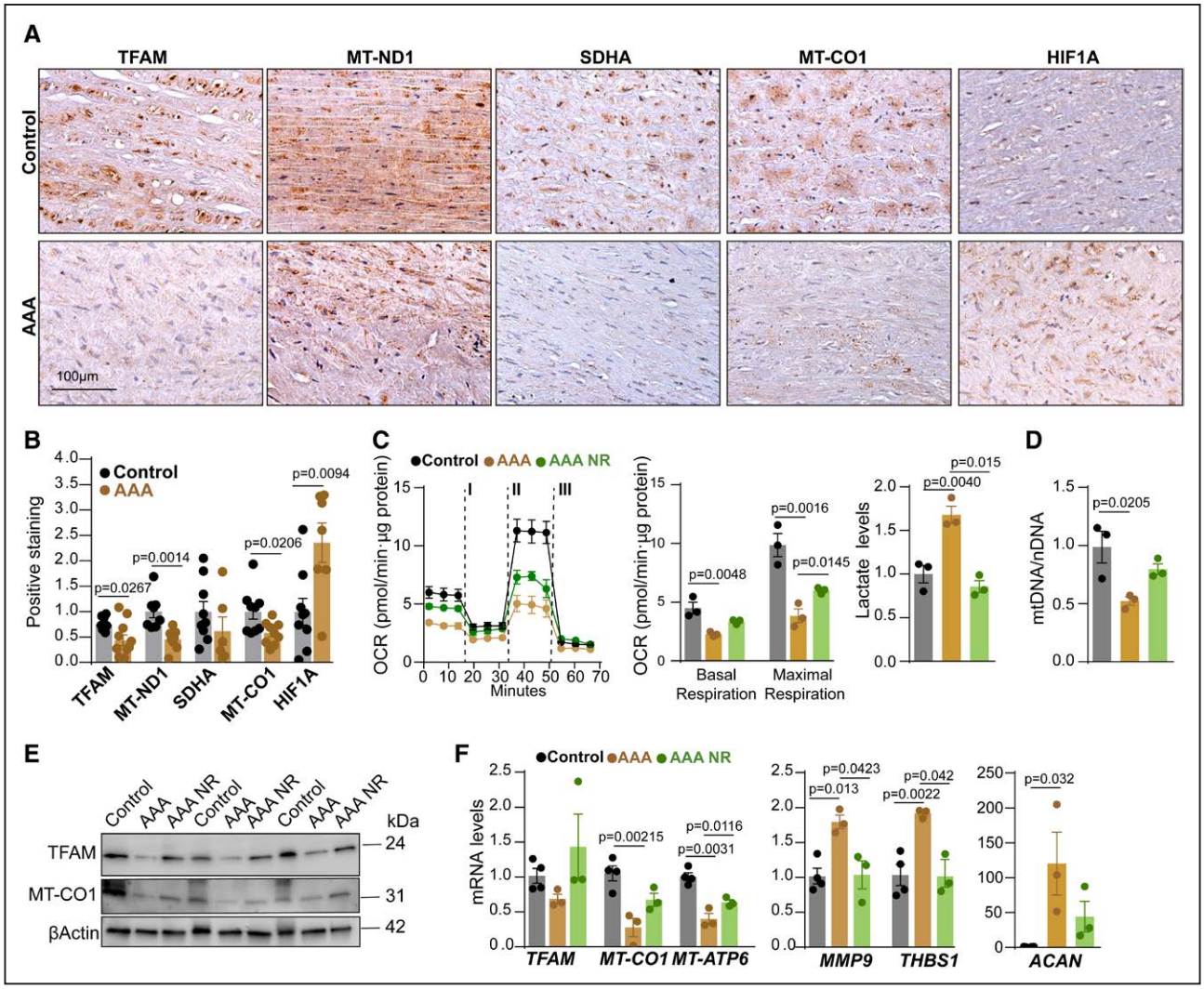

Figure 2. Mitochondrial respiration decline in human atherosclerotic abdominal aortic aneurysm.
A, Immunohistochemical analysis and (**B**) quantification, in human atherosclerotic abdominal aortic aneurysms (AAA) samples from patients and control donors (n=9 each group). **C**, Oxygen consumption rate (OCR; Seahorse Biosciences) in vehicle- and NR-treated in medial VSMCs from human control (n=4) and AAAs (n=4) at basal respiration and after addition of oligomycin (I) and fluoro carbonyl cyanide phenylhydrazone (II) to measure maximal respiration, followed by a combination of rotenone and antimycin A (III); normalized extracellular lactate levels measured by reagent strips for Accutrend Plus Lactate Pro (Roche). **D**, qPCR analysis of relative mtDNA levels (*MT-CO1*) relative to nuclear DNA (*B2M*). **E**, Immunoblot analysis of TFAM and MT-CO1 from aortic medial VSMCs for AAA patients and Controls (n=4 for each group), β-Actin was used for loading control. **F**, qPCR analysis of relative *TFAM, MT-CO1, MT-ATP6*, *MMP9*, *THBS1* and *ACAN* mRNA expression. Values are expressed as mean±SEM. Normality of data was checked using Shapiro-Wilk test. *F*-test was used to assess the equality of variance assumption. Differences between 2 groups were assessed using unpaired Student *t*-test, or *t*-test with Welch correction for unequal variances, where appropriate. Differences between the 3 groups were assessed by using 1-way ANOVA and a Tukey multiple comparisons test.

point to convergent pathways and therapeutic strategies for both, hereditable and atherosclerotic aortic aneurysms. We have previously described that the mitochondrial function of aortic VSMCs is altered in a mouse model of Marfan syndrome and human samples, and the treatment with NR enhances mitochondrial respiration and reverts the aortic pathology. Moreover, forcing mitochondrial failure in VSMCs by conditional depletion of Tfam induces the development of aortic aneurysms and precipitate premature death because of aortic ruptures.[7] Here, we show that VSMCs from patients with atherosclerotic aortic aneurysm exhibit reduced TFAM expression and mitochondrial respiration as occurs in VSMCs from Marfan syndrome patients, suggesting that beside their different etiology, mitochondrial dysfunction is a hallmark of aortic dilation and VSMCs-dysfunction in both hereditable and atherosclerotic aortic aneurysm diseases. According with these results, previous studies have found altered mitochondrial morphology and function in atherosclerotic aortic aneurysms.[8,9,17] Further studies are required to elucidate exactly how aneurysms with different etiologies of AAD converge on the impairment of TFAM expression and mitochondrial dysfunction.

Beside controlling the energetic status, cellular metabolism modulates key metabolites that serve as cofactors or substrates for the enzymatic reactions that catalyze the epigenetic modifications and transcriptional regulation. Recent evidences support the coordination between metabolism and epigenetic landscape in VSMC function and proliferation during microvascular diseases and pulmonary hypertension.[18]

In this work, we show that boosting vascular metabolism with NAD^+-precursors reduces the expression of synthetic genes, prevents AA-development and fatal aortic ruptures in hypercholesterolemic ApoE-deficient mice. Accordingly, a previous report showed that increasing NAD^+ levels with niacin, prevents aortic dilation in mice by promoting Sirtuin-1 activity.[19] Mitochondria-specific autophagy (mitophagy), a cellular catabolic process targeting damaged mitochondria, holds a prominent role in mitochondrial quality control[20] and is dysregulated in aortic aneurysms.[21,22] Chen et al[23] showed that both treatment with NR or with metformin, an antidiabetic drug that enhances autophagy, rescued mitophagy defects and mitochondrial function in mitochondrial DNA polymerase gamma (POLG)-mutant cells. In fact, there is strong evidence about the protective effect of metformin on abdominal aortic aneurysm growth and rupture in humans and ApoE-mouse models.[24,25] Wang et al[26] found that pharmacological metformin concentration improves mitochondrial respiration by increasing mitochondrial fission through AMPK-mitofusin signaling. However, the mechanism of metformin action, in particular, in mitochondrial metabolism, remains controversial and appears to be dose dependent. Indeed, supraphar-macological metformin concentrations reduced mitochondrial respiration by decreasing adenine nucleotide levels.[24,26] Hence, metformin, as NR, might improve VSMC function by enhancing mitochondrial metabolism and by triggering mitophagy.

The formation of an AAD is a progressive process in which multiple pathways are sequentially activated. Importantly, in this work, we confirm that NR treatment is effective when given after the onset of the development of the atherosclerotic AAD, suggesting that it could hold curative, and not only, preventive potential. Accordingly, we previously reported that NR treatment in Marfan mice already presenting aortic enlargement and medial degeneration is able to reduce the aortic diameter, to improve aortic histology and to revert the pathological transcriptional signature of VSMCs. Therefore, NR treatment holds prophylactic and curative capacity in both, atherosclerotic and genetic AAD mouse models. Altogether, these evidence highlight the pivotal role of vascular metabolism and mitochondrial function in aortic aneurysms and ruptures independently of their aetiology and unravel nicotinamide precursors as molecules with potential curative properties, opening an immense avenue of therapeutic opportunities.

ARTICLE INFORMATION

Received July 20, 2021; accepted February 9, 2022.

Affiliations

Centro de Biología Molecular Severo Ochoa (CBMSO), Consejo Superior de Investigaciones Científicas (CSIC)-Universidad Autónoma de Madrid (UAM), Madrid, Spain (J.O., E.G.-R., M.M.). Instituto de Investigación Sanitaria del Hospital 12 de Octubre (i+12), Madrid, Spain (J.O., E.G.-R., M.M.). Centro de Investigación Biomédica en Red de Enfermedades Cardiovasculares (CIBER-CV), Spain (J.O., R.R.-M. M.J.R.-R., J.M.R., J.L.M.-V.). Instituto de Investigación Sanitaria Fundación Jiménez Díaz, Madrid, Spain (R.R.-M., J.L.M.-V.). Centro Nacional de Investigaciones Cardiovasculares Carlos III (CNIC), Madrid, Spain (M.J.R.-R., J.M.R.).

Acknowledgments

J. Oller and M. Mittelbrunn designed the research. J. Oller performed most of the experiments and analyzed the data. E. Gabandé-Rodríguez, R. Roldan-Montero, and M. Jesús Ruiz-Rodríguez provided experimental and technical support. J. Luís Martín-Ventura and J. Miguel Redondo provided reagents. J. Oller, E. Gabandé-Rodríguez, and M. Mittelbrunn wrote the article.

Sources of Funding

This study was supported by the Fondo de Investigación Sanitaria del Instituto de Salud Carlos III (PI16/188, PI19/855), the European Regional Development Fund (ERDF), and the European Commission through H2020-EU.1.1 and European Research Council grant ERC-2016-StG 715322-EndoMitTalk. This work was partially supported by Comunidad de Madrid (S2017/BMD-3867 RENIM-CM), co-financed by European Structural and Investment Fund. M. Mittelbrunn is supported by the Miguel Servet Program (CP 19/014, Fundación de Investigación del Hospital 12 de Octubre). J. Oller and E. Gabandé-Rodríguez are supported by Juan de la Cierva (IJC2019-040152-I and IJC2018-036850-I respectively). Support was also provided by Ministerio de Ciencia e Innovación grants (RTI2018-099246-B-I00, Comunidad de Madrid and Fondo Social Europeo funds (AORTASANA-CM; J. Miguel Redondo), J. Miguel Redondo was also funded by Fundación La Caixa (HR18-00068), The Marfan Foundation USA and the CIBER-CV of Ministerio de Ciencia e Innovación (CB16/11/00264).

Disclosures

None.

Supplemental Material

Expanded Materials and Methods
Table S1

REFERENCES

1. Golledge J, Eagle KA. Acute aortic dissection. *Lancet.* 2008;372:55–66. doi: 10.1016/S0140-6736(08)60994-0
2. Pinard A, Jones GT, Milewicz DM. Genetics of thoracic and abdominal aortic diseases. *Circ Res.* 2019;124:588–606. doi: 10.1161/CIRCRESAHA.118.312436
3. Nordon IM, Hinchliffe RJ, Loftus IM, Thompson MM. Pathophysiology and epidemiology of abdominal aortic aneurysms. *Nat Rev Cardiol.* 2011;8:92–102. doi: 10.1038/nrcardio.2010.180
4. Dzobo KE, Hanford KML, Kroon J. Vascular metabolism as driver of atherosclerosis: linking endothelial metabolism to inflammation. *Immunometabolism.* 2021;3:e210020. doi: 10.20900/immunometab20210020
5. Pi X, Xie L, Patterson C. Emerging roles of vascular endothelium in metabolic homeostasis. *Circ Res.* 2018;123:477–494. doi: 10.1161/CIRCRESAHA.118.313237
6. Shi J, Yang Y, Cheng A, Xu G, He F. Metabolism of vascular smooth muscle cells in vascular diseases. *Am J Physiol Heart Circ Physiol.* 2020;319:H613–H631. doi: 10.1152/ajpheart.00220.2020
7. Oller J, Gabandé-Rodríguez E, Ruiz-Rodríguez MJ, Desdín-Micó G, Aranda JF, Rodrigues-Diez R, Ballesteros-Martínez C, Blanco EM, Roldan-Montero R, Acuña P, et al. Extracellular tuning of mitochondrial respiration leads to aortic aneurysm. *Circulation.* 2021;143:2091–2109. doi: 10.1161/CIRCULATIONAHA.120.051171
8. Gutierrez PS, Piubelli MLM, Naal KG, Dias RR, Borges LF. Mitochondria in aneurysms and dissections of the human ascending aorta. *Cardiovasc Pathol.* 2020;47:107207. doi: 10.1016/j.carpath.2020.107207

9. Tang L, Cong Z, Hao S, Li P, Huang H, Shen Y, Li K, Jing H. Protective effect of melatonin on the development of abdominal aortic aneurysm in a rat model. *J Surg Res.* 2017;209:266–278.e1. doi: 10.1016/j.jss.2016.06.018
10. Fashandi AZ, Spinosa M, Salmon M, Su G, Montgomery W, Mast A, Lu G, Hawkins RB, Cullen JM, Sharma AK, et al. Female mice exhibit abdominal aortic aneurysm protection in an established rupture model. *J Surg Res.* 2020;247:387–396. doi: 10.1016/j.jss.2019.10.004
11. Henriques TA, Huang J, D'Souza SS, Daugherty A, Cassis LA. Orchidectomy, but not ovariectomy, regulates angiotensin II-induced vascular diseases in apolipoprotein E-deficient mice. *Endocrinology.* 2004;145:3866–3872. doi: 10.1210/en.2003-1615
12. Oller J, Méndez-Barbero N, Ruiz EJ, Villahoz S, Renard M, Canelas LI, Briones AM, Alberca R, Lozano-Vidal N, Hurlé MA, et al. Nitric oxide mediates aortic disease in mice deficient in the metalloprotease Adamts1 and in a mouse model of Marfan syndrome. *Nat Med.* 2017;23:200–212. doi: 10.1038/nm.4266
13. Guedj K, Khallou-Laschet J, Clement M, Morvan M, Delbosc S, Gaston AT, Andreata F, Castier Y, Deschildre C, Michel JB, et al. Inflammatory microenvironmental cues of human atherothrombotic arteries confer to vascular smooth muscle cells the capacity to trigger lymphoid neogenesis. *PLoS One.* 2014;9:e116295. doi: 10.1371/journal.pone.0116295
14. Amin HZ, Sasaki N, Yamashita T, Mizoguchi T, Hayashi T, Emoto T, Matsumoto T, Yoshida N, Tabata T, Horibe S, et al. CTLA-4 protects against angiotensin II-induced abdominal aortic aneurysm formation in mice. *Sci Rep.* 2019;9:8065. doi: 10.1038/s41598-019-44523-6
15. Trachet B, Aslanidou L, Piersigilli A, Fraga-Silva RA, Sordet-Dessimoz J, Villanueva-Perez P, Stampanoni MFM, Stergiopulos N, Segers P. Angiotensin II infusion into ApoE-/- mice: a model for aortic dissection rather than abdominal aortic aneurysm? *Cardiovasc Res.* 2017;113:1230–1242. doi: 10.1093/cvr/cvx128
16. Saraff K, Babamusta F, Cassis LA, Daugherty A. Aortic dissection precedes formation of aneurysms and atherosclerosis in angiotensin II-infused, apolipoprotein E-deficient mice. *Arterioscler Thromb Vasc Biol.* 2003;23:1621–1626. doi: 10.1161/01.ATV.0000085631.76095.64
17. Sobenin IA, Sazonova MA, Postnov AY, Bobryshev YV, Orekhov AN. Changes of mitochondria in atherosclerosis: possible determinant in the pathogenesis of the disease. *Atherosclerosis.* 2013;227:283–288. doi: 10.1016/j.atherosclerosis.2013.01.006
18. Li D, Shao NY, Moonen JR, Zhao Z, Shi M, Otsuki S, Wang L, Nguyen T, Yan E, Marciano DP, et al. ALDH1A3 coordinates metabolism with gene regulation in pulmonary arterial hypertension. *Circulation.* 2021;143:2074–2090. doi: 10.1161/CIRCULATIONAHA.120.048845
19. Horimatsu T, Blomkalns AL, Ogbi M, Moses M, Kim D, Patel S, Gilreath N, Reid L, Benson TW, Pye J, et al. Niacin protects against abdominal aortic aneurysm formation via GPR109A independent mechanisms: role of NAD+/nicotinamide. *Cardiovasc Res.* 2020;116:2226–2238. doi: 10.1093/cvr/cvz303
20. Chen G, Kroemer G, Kepp O. Mitophagy: an emerging role in aging and age-associated diseases. *Front Cell Dev Biol.* 2020;8:200. doi: 10.3389/fcell.2020.00200
21. Ramadan A, Singh KK, Quan A, Plant PJ, Al-Omran M, Teoh H, Verma S. Loss of vascular smooth muscle cell autophagy exacerbates angiotensin II-associated aortic remodeling. *J Vasc Surg.* 2018;68:859–871. doi: 10.1016/j.jvs.2017.08.086
22. Ramadan A, Al-Omran M, Verma S. The putative role of autophagy in the pathogenesis of abdominal aortic aneurysms. *Atherosclerosis.* 2017;257:288–296. doi: 10.1016/j.atherosclerosis.2017.01.017
23. Chen A, Kristiansen CK, Hong Y, Kianian A, Fang EF, Sullivan GJ, Wang J, Li X, Bindoff LA, Liang KX. Nicotinamide riboside and metformin ameliorate mitophagy defect in induced pluripotent stem cell-derived astrocytes with POLG mutations. *Front Cell Dev Biol.* 2021;9:737304. doi: 10.3389/fcell.2021.737304
24. Wang Z, Guo J, Han X, Xue M, Wang W, Mi L, Sheng Y, Ma C, Wu J, Wu X. Metformin represses the pathophysiology of AAA by suppressing the activation of PI3K/AKT/mTOR/autophagy pathway in ApoE-/- mice. *Cell Biosci.* 2019;9:68. doi: 10.1186/s13578-019-0332-9
25. Yuan Z, Heng Z, Lu Y, Wei J, Cai Z. The protective effect of metformin on abdominal aortic aneurysm: a systematic review and meta-analysis. *Front Endocrinol (Lausanne).* 2021;12:721213. doi: 10.3389/fendo.2021.721213
26. Wang Y, An H, Liu T, Qin C, Sesaki H, Guo S, Radovick S, Hussain M, Maheshwari A, Wondisford FE, et al. Metformin improves mitochondrial respiratory activity through activation of AMPK. *Cell Rep.* 2019;29:1511 e5–1523 e5. doi: 10.1016/j.celrep.2019.09.070